density type tumors had limited cardiopulmonary reserve; lymph node exploration was considered not to be beneficial mainly because of calcified nodes, dense pleural adhesion, and hypoxemia during operation.

Histopathologically, none of the patients with air-containing type tumors had vascular invasion or pleural involvement; however, 8 (17%) were given a diagnosis of not pure BAC (adenocarcinoma with mixed subtypes) because of minimal stromal invasion. In contrast, all solid-density type tumors were non-BACs associated with high rates (47% of all solid-density type tumors) of pleural involvement or vascular invasion.

There were no serious complications after operation and no surgical mortality. Two patients with air-containing type tumors and 1 with a solid-density type tumor died of other diseases, with no evidence of recurrence. Seven patients with solid-density type tumors died of recurrent lung cancer; the first site of recurrence was locoregional in 5 patients (3 wedge resections, 2 segmentectomies) and liver metastasis in 2 (1 wedge resection, 1 segmentectomy). The sites of locoregional recurrence were pleural dissemination in 2 patients (1 wedge resection, 1 segmentectomy), pulmonary metastasis in 2 (1 wedge resection, 1 segmentectomy), and mediastinal lymph node in 1 (wedge resection). No patient with air-containing type tumors had recurrence. Overall and relapse-free survival curves are shown in Figures 3 and 4. Median follow-up of the survivors was 70 months (range, 21 to 133 months) in patients with air-containing type tumors and 49 months (range, 25 to 112 months) in those with solid-density type tumors. Overall and relapse-free survival rates at 5 years were 95% and 100%, respectively, in patients with air-containing type tumors, as compared with 69% and 57%, respectively, in those with solid-density type tumors. Both survival rates were significantly better in patients with air-containing type tumors than in those with solid-density type tumors ($p < 0.0001$).

Comment

Lobectomy remains the standard operation for small non–small-cell lung cancers. The role of intentional sublobar resection for these tumors should be evaluated in well-designed clinical trials. At present, there are two possible indications for intentional sublobar resection. The first is for clinically diagnosed very early lung cancers, usually defined as clinical T1 N0 M0 tumors 2 cm or less in diameter that are located in the periphery of the lung. Because lymph node metastasis accompanies approximately 15% of adenocarcinomas of this size [12], N0 status must be confirmed at operation. In most series of patients undergoing sublobar resection for clinically very early lung cancers, segmental resection is the procedure of choice to gain access to the hilar lymph nodes [2–4]. In addition, segmentectomy for confirming N0 status should be selected in the patients with adenocarcinomas of solid-density type on HRCT because nodal involvement was found in 12% of these patients [7].

The other possible indication for intentional sublobar resection is pathologically confirmed noninvasive adenocarcinoma of the lung. The histologic classification of the World Health Organization defines BAC as noninvasive adenocarcinoma showing pure lepidic growth without vascular, stromal, or pleural invasion [9]. Lymph node metastasis has not been found in patients with BAC, and cure is likely after complete resection [5]. An improved understanding of the pathologic characteristics of peripheral lung adenocarcinoma and increased use of CT scanning has led interest to focus on the correlation of CT images with the histologic features of BAC. Attempts have been made to identify CT findings that could serve as landmarks for sublobar resection [6–8, 13–18]. Bronchioloalveolar carcinoma components showing lepidic growth along alveoli, without areas of invasion, present as areas of GGO on HRCT [14]. The proportion of GGO is directly related to tumor histology and behavior. Patients with adenocarcinomas measuring 2 cm or less in which the proportion of GGO to the whole tumor area on HRCT was 50% or greater have no lymph node involvement and survive without any recurrence after resection [13, 15]. The TDR on HRCT images is also a simple and useful index for identifying early adenocarcinoma of the lung [7, 8, 16]. Visual evaluation of the GGO ratio is subject to considerable variability among examiners [18]. In contrast, evaluation of the TDR on HRCT has the advantage of simplicity and does not require the use of complex instrumentation: tumor opacity on lung window images is simply compared with that on mediastinal images [7]. Okada and colleagues [16] reported that the extent of both TDR and GGO correlate well with that of the BAC growth of adenocarcinomas; however, the TDR more strongly correlates with the BAC proportion than does the GGO ratio. Previously, we also reported that adenocarcinomas measuring 2 cm or less in diameter in which the TDR on HRCT was 50% or greater have no lymph node involvement and rarely show microscopic invasion. These findings suggested that sublobar resection might be an appropriate approach for the management of such tumors [7, 8]. Few studies have evaluated the outcomes of sublobar resections performed on the basis of HRCT characteristics other than pure GGO. We therefore retrospectively investigated surgical outcomes in patients who underwent sublobar resections according to findings on preoperative HRCT images.

The outcomes of sublobar resection for these possibly indolent tumors should be assessed on the basis of long-term disease-free survival and recurrence patterns. We therefore excluded patients who had a history of previous primary lung cancers or other malignancies, as well as those with multiple lung cancers. About half of the initially screened patients with these small-sized adenocarcinomas of the lung who underwent sublobar resection were excluded. In our series, all patients with air-containing type tumors, excluding 2 who died of other diseases, survived with no evidence of recurrence, despite incomplete lymph node exploration. Sublobar resections for these air-containing type tumors did not require lymph node sampling or dissection, and the

extent of resection depended on only lesion size or location. In addition, not all of the air-containing type lesions were diagnosed as BAC, whereas 8 (17%) were diagnosed as mixed adenocarcinomas with minimal stromal invasion. Those patients who had BAC with focal or minimal invasion survived with no relapse for 41 to 82 months (median, 51 months) after operation. This result suggested that some patients with radiologic evidence of early lung adenocarcinoma on the basis of TDR show minimal invasion on pathologic examination and might be cured by sublobar resection. However, this point remains controversial, and further studies are needed.

In conclusion, our results suggest that the TDR on HRCT images is a simple and useful variable for identifying small adenocarcinomas indicated for limited pulmonary resection. The outcome of sublobar resection for air-containing type lesions may be favorable in patients with curable disease. Larger, multicenter trials are needed to identify HRCT images that more precisely reflect the biologic behavior of these tumors and to assess the surgical outcomes of sublobar resection indicated on the basis of these HRCT images.

This work was supported in part by a grant-in-aid for cancer research (grant 15-1) from the Ministry of Health, Labor and Welfare, Japan.

References

1. Ginsberg RJ, Rubinstein LV. Randomized trial of lobectomy versus limited resection for T1N0 non-small cell lung cancer. Lung Cancer Study Group. Ann Thorac Surg 1995;60:615–23.
2. Kodama K, Doi O, Higashiyama M, Yokouchi H. Intentional limited resection for selected patients with T1N0M0 non-small-cell lung cancer: a single-institution study. J Thorac Cardiovasc Surg 1997;114:347–53.
3. Yoshikawa K, Tsubota N, Kodama K, Ayabe H, Taki T, Mori T. Prospective study of extended segmentectomy for small lung tumors: the final report. Ann Thorac Surg 2002;73: 1055–9.
4. Okada M, Koike T, Higashiyama M, Yamato Y, Kodama K, Tsubota N. Radical sublobar resection for small-sized non-small cell lung cancer: a multicenter study. J Thorac Cardiovasc Surg 2006;132:769–75.
5. Noguchi M, Morikawa A, Kawasaki M, et al. Small adenocarcinoma of the lung. Histologic characteristics and prognosis. Cancer 1995;75:2844–52.
6. Travis WD, Garg K, Franklin WA, et al. Evolving concepts in the pathology and computed tomography imaging of lung adenocarcinoma and bronchioloalveolar carcinoma. J Clin Oncol 2005;23:3279–87.
7. Kondo T, Yamada K, Noda K, Nakayama H, Kameda Y. Radiologic-prognostic correlation in patents with small pulmonary adenocarcinomas. Lung Cancer 2002;36:49–57.
8. Shimizu K, Yamada K, Saito H, et al. Surgically curable peripheral lung carcinoma: correlation of thin-section CT findings with histologic prognostic factors and survival. Chest 2005;127:871–8.
9. Travis WD, Colby TV, Corrin B, Shimosato Y, Brambilla E. Histologic typing of lung and pleural tumours. World Health Organization international histological classification of tumours. Berlin: Springer, 1999.
10. Sobin LH, Wittekind Ch, eds. International Union Against Cancer (UICC): TNM classification of malignant tumors, 6th ed. New York: Wiley-Liss, 2002.
11. The Japan Lung Cancer Society. Classification of lung cancer, 1st English ed. Tokyo: Kanahara, 2000.
12. Asamura H, Nakayama H, Kondo H, Tsuchiya R, Shimosato Y, Naruke T. Lymph node involvement, recurrence, and prognosis in resected small, peripheral, non-small-cell carcinomas: are these carcinomas candidates for video-assisted lobectomy? J Thorac Cardiovasc Surg 1996;111:1125–34.
13. Kodama K, Higashiyama M, Yokouchi H, et al. Prognostic value of ground-glass opacity found in small lung adenocarcinoma on high-resolution CT scanning. Lung Cancer 2001; 33:17–25.
14. Kuriyama K, Seto M, Kasugai T, et al. Ground-glass opacity on thin-section CT: value in differentiating subtypes of adenocarcinoma. AJR Am J Roentgenol 1999;173:465–9.
15. Matsuguma H, Yokoi K, Anraku M, et al. Proportion of ground-glass opacity on high-resolution computed tomography in clinical T1 N0 M0 adenocarcinoma of the lung: a predictor of lymph node metastasis. J Thorac Cardiovasc Surg 2002;124:278–84.
16. Okada M, Nishio W, Sakamoto T, et al. Correlation between computed tomographic findings, bronchioloalveolar carcinoma component, and biologic behavior of small-sized lung adenocarcinoma. J Thorac Cardiovasc Surg 2004;127:857–61.
17. Suzuki K, Kusumoto M, Watanabe S, Tsuchiya R, Asamura H. Radiologic classification of small adenocarcinoma of the lung: radiologic-pathologic correlation and its prognosis. Ann Thorac Surg 2006;81:413–20.
18. Nakata M, Sawada S, Yamashita M, et al. Objective radiologic analysis of ground-glass opacity aimed at curative limited resection for small peripheral non-small cell lung cancer. J Thorac Cardiovasc Surg 2005;129:1226–31.

Phase II Study of Paclitaxel and Irinotecan Chemotherapy in Patients With Advanced Nonsmall Cell Lung Cancer

Fumihiro Oshita, MD, Haruhiro Saito, MD, Kouzo Yamada, MD, and Kazumasa Noda, MD

Objectives: We conducted a phase II study of combination chemotherapy with paclitaxel (Pac) and irinotecan (CPT) to determine the qualitative and quantitative toxicities and efficacy of the combination against advanced nonsmall cell lung cancer (NSCLC).

Patients and Methods: Patients with stage IIIB or IV NSCLC were treated with CPT at 60 mg/m^2 and Pac at 160 mg/m^2 every 2 weeks.

Results: Between May 2002 and July 2004, 39 of registered 46 patients received 4 to 6 cycles of chemotherapy, and 7 patients discontinued treatment because of disease progression in 5 patients and grade 2 pneumonitis in 2 patients. Grade 3 anemia, leukopenia, neutropenia, and elevation of bilirubin occurred in 4.0%, 0.5%, 1.0%, and 0.5%, respectively. Twenty-one patients responded, and the overall response rate was 45.6%. The median survival time was 355 days and the 1-year survival rate was 47.8%.

Conclusion: Pac plus CPT was efficacious and safe in NSCLC.

Key Words: paclitaxel, irinotecan, nonsmall cell, lung cancer

(*Am J Clin Oncol* 2007;30: 358–360)

Current chemotherapy regimens for metastatic nonsmall cell lung cancer (NSCLC) are not particularly effective, and the disease cannot be cured even with the most effective chemotherapy. Current international guidelines recommend the use of platinum-based chemotherapy for patients with advanced NSCLC,[1] and the use of doublets including platinum plus a third-generation agent has been widely accepted for patients with a good performance status. A meta-analysis of the published literature clearly showed the superiority of platinum-containing regimens in terms of objective response rate, and this superiority was found throughout the subgroup analyses performed.[2] The study results also confirmed that platinum-based therapy is generally associated with higher toxicity, particularly nausea and vomiting, hematologic toxicity, and nephrotoxicity. Nevertheless, platinum-based regimens can be administered as safely as nonplatinum therapies when patients are selected correctly. However, this study did not include every combination of nonplatinum drugs, and it is necessary to examine every such new combination for efficacy and toxicity.

Combined analysis of two randomized phase III studies demonstrated that irinotecan (CPT) combined with cisplatin significantly improves survival compared with vindesine and cisplatin in patients with advanced NSCLC.[3] In Japan, CPT is considered a key drug against NSCLC. Preclinical studies that have evaluated combinations of a camptothecin with a taxane have yielded promising results, and several studies have demonstrated an additive or synergistic interaction between camptothecin and taxanes.[4] Our previous phase I study of a Pac and CPT combination showed that pneumonitis was the dose-limiting toxicity and led to a recommendation of Pac 160 mg/m^2 and CPT 60 mg/m^2 every 2 weeks for further study.[5] This study also demonstrated an objective response rate of 58.3% and a 1-year survival rate of 54.2%. Accordingly, we expected the combination of Pac and CPT to display high activity against NSCLC and designed a phase II study to determine the efficacy and toxicities.

PATIENTS AND METHODS

The Institutional Review Board of Kanagawa Cancer Center reviewed and approved this study prior to commencement.

Patients

Patients with histologically or cytologically confirmed NSCLC were registered. Eligibility criteria were: clinical stage IIIB or IV, an expected survival of at least 12 weeks, age <70 years, Eastern Cooperative Oncology Group PS score ≤1, leukocyte count ≥4000/μL, hemoglobin ≥10 g/dL, platelet count ≥100,000/μL, total serum bilirubin ≤1.5 mg/dL, aspartate aminotransferase and alanine aminotransferase ≤90 IU/L, and serum creatinine ≤1.5 mg/dL. Patients who had experienced postoperative recurrence were eligible for this study, but a 4 or more week rest period was required after surgery. Patients who had received chemotherapy or radiotherapy were excluded from this study. Written informed consent was obtained from every patient.

Chemotherapy

All patients without disease progression were treated every 2 weeks for a total of 4 courses of chemotherapy. CPT was administered at a dose of 60 mg/m^2 on day 1. Pac was administered at a dose of 160 mg/m^2 on day 1. Premedication

From the Department of Thoracic Oncology, Kanagawa Cancer Center, Yokohama, Japan.

Supported in part by the Kanagawa Prefectural Hospitals Cancer Research Fund and Kanagawa Health Foundation.

Reprints: Fumihiro Oshita, MD, Department of Thoracic Oncology, Kanagawa Cancer Center, Nakao 1-1-2, Asahi-ku, Yokohama 241-0815, Japan. E-mail: foshita@kcch.jp.

ISSN: 0277-3732/07/3004-0358
DOI: 10.1097/01.coc.0000258091.25459.d1

consisting of 20 mg dexamethasone and 50 mg ranitidine was infused. A 50-mg oral dose of diphenhydramine was also administered. Prophylactic G-CSF, 50 $\mu g/m^2$ per day or 2 $\mu g/kg$ per day, was administered subcutaneously on days 6 to 10. Patients were given a 5-HT_3 antagonist intravenously. Subsequent courses of chemotherapy were started when patients satisfied the organ function criteria: leukocyte count $\geq 3000/\mu L$, neutrophil count $\geq 1500/\mu L$, platelet count $\geq 75{,}000/\mu L$, and less than grade 1 nonhematologic toxicities, except alopecia. Grade 3 nausea and vomiting did not preclude subsequent courses of chemotherapy. Chemotherapy was repeated for a maximum of 6 courses unless the disease progressed, but it was stopped if the tumor response was judged to be NC after 4 courses. Tumor response was evaluated according to RECIST criteria.[6] Toxicities were evaluated according to the NCI-CTC (version 2) criteria.[7]

Study Design

We chose a 50% response rate as a desirable target level and a 30% response rate as uninteresting. The study design had power in excess of 90% and less than 10% error; therefore, 22 assessable patients in the first step and 24 in the second step were required according to the optimal design of Simon.[8] We decided to stop the study if there were fewer than 8 responders in the first step. The regimen was defined as active if there were 18 or more responders out of the total of 46 patients. Overall survival was estimated by the method of Kaplan and Meier.

RESULTS

Between May 2002 and July 2004, 46 patients were registered in the phase II study (Table 1). A total of 22 patients were registered for assessment of response in the first stage. Nine of 22 patients in the first stage responded and 24 patients were registered in the second stage. A total of 198 cycles was administered to 46 patients. Thirty-nine patients received 4 to 6 cycles of chemotherapy, except for 7 patients who discontinued treatment in the first or second cycles because of disease progression in 5 patients and grade 2 pneumonitis with pulmonary infiltration in 2 patients. Adverse effects and events are summarized in Table 2. Grade 3 anemia, leukopenia, neutropenia, and elevation of bilirubin occurred in 4.0%, 0.5%, 1.0%, and 0.5%, respectively. There were no grade 4 toxicities.

Twenty-one of 46 patients achieved partial response, 18 no change, 6 progressive disease, and 1 not evaluated, and the overall response rate was 45.6% in phase II study. The median duration of partial response was 154 days (range, 76–380 days). The median survival time was 355 days and the 1-year survival rate was 47.8% (Table 3). The outcome in 70 patients including those from the phase I study (5) demonstrated that 1 patient achieved complete response, 34 PR, and the overall response rate was 50.0%. The median survival time was 361 days and the 1-year survival rate was 50.0%.

DISCUSSION

The objective response rate of 50.0% and 1-year survival rate of 50.0% with our nonplatinum Pac and CPT regimen in 70 patients in phase I and phase II studies are somewhat better than in a large phase III trial of 4 platinum-based chemotherapy regimens, which showed response rates of 17% to 22% and 1-year survival rates of 31% to 34%.[9] The

TABLE 1. Patient Characteristics

Characteristic	Value
Total	46
Age (years)	
Median	61
Range	43–69
Gender (no. patients)	
Male	29
Female	17
Performance status (ECOG) (no. patients)	
0	12
1	34
Clinical stage (no. patients)	
IIIB	6
IV	34
Postoperative recurrence	6
Histology (no. patients)	
Adenocarcinoma	36
Others	10
No. metastatic organs (no. patients)	
1	27
≥2	13
Brain metastasis (no. patients)	8

TABLE 2. Adverse Effects and Events

	NCI-CTC Grade (No. Cycles)					
Toxicity	0	1	2	3	4	% ≥Grade 3
Hemoglobin	29	137	24	8	0	4.0
Leukocyte	162	23	12	1	0	0.5
Neutrophil	167	19	10	2	0	1.0
Platelets	188	10	0	0	0	—
Bilirubin	165	22	10	1	0	0.5
Creatinine	192	6	0	0	0	—
SGOT	146	51	1	0	0	—
SGPT	135	55	8	0	0	—
Infection	194	3	1	0	0	—
Nausea/vomiting	143	51	4	0	0	—
Diarrhea	165	31	2	0	0	—
Myalgia	97	76	25	0	0	—
Arthralgia	110	64	24	0	0	—
Neuropathy	107	76	15	0	0	—
Fever	183	14	1	0	0	—
Allergic reaction	195	3	0	0	0	—
Alopecia	95	79	24	0	0	—
Pneumonitis	196	0	2	0	0	—
Hypotension	193	5	0	0	0	—
Arrhythmia	194	4	0	0	0	—

NCI-CTC, National Cancer Institute-Common Toxicity Criteria (version 2).

TABLE 3. Therapeutic Outcome in Phase II Study

Response	No. Patients
Complete response	0
Partial response	21
No change	18
Progressive disease	6
Not evaluated	1
Response rate (%)	45.6
Median survival time (days)	355
% of 1-year survivor	47.8

antitumor activity of the Pac and CPT combination is thought to be attributable to a synergistic action between these drugs. A possible mechanism of the synergy is a drug-drug interaction, such as that shown in a pharmacokinetic study that demonstrated elevation of the AUC of CPT and SN-38 by Pac infusion.[10] Although we acknowledge the possibility that Pac and CPT might affect each other's pharmacokinetics, increasing their activity against NSCLC, we also considered that another possible mechanism for this high activity of the Pac and CPT combination might be related to influx and efflux in the cell system. The combination of Pac and SN-38 down-regulates the level of multidrug resistance-associated protein, which may be an efflux pump for cisplatin, in ovarian cancer cell lines, suggesting that this combination will overcome drug resistance.[11]

The combination of Pac and CPT also appears useful in that little toxicity was observed in this study. No patients experienced grade 4 toxicities. All patients, except the 5 patients who developed disease progression during treatment and the 2 patients who experienced grade 2 pneumonitis with pulmonary infiltration, were able to receive 4 to 6 cycles of this therapy. The pneumonitis was thought to be attributable to a booster effect of an allergic reaction when 180 mg/m^2 or higher of Pac was combined with CPT in the phase I study, but no patients experienced pneumonitis during cycles 2 to 6 of chemotherapy in this phase II study. Therefore, pneumonitis was seen at a frequency similar to that in other combination chemotherapies. Neutropenia was mild because of the prophylactic use of G-CSF in this study. We used G-CSF when monocytopenia less than 150/μL appeared in the phase I study,[5] and most patients received G-CSF for 5 days starting on days 5, 6, or 7. Consequently, G-CSF was given routinely for 5 days from day 5 to day 9 in every cycle in the present study. This less toxic regimen may be helpful in the treatment of high-risk patients, such as the elderly or those with poor performance status or moderately severe complications.

REFERENCES

1. American Society of Clinical Oncology. Treatment of unresectable non-small cell lung cancer guideline: update 2003. *J Clin Oncol.* 2004; 22:330–353.
2. D'Addario G, Pintile M, Leighl NB, et al. Platinum-based versus non-platinum-based chemotherapy in advanced non-small-cell lung cancer: a meta-analysis of the published literature. *J Clin Oncol.* 2005;23: 2926–2936.
3. Negoro S, Masuda N, Takada Y, et al. Randomized phase III trial of irinotecan combined with cisplatin for advanced non-small cell lung cancer. *Br J Cancer.* 2003;88:335–341.
4. Fukuda M, Nishio K, Shiraishi J, et al. Effects of combinations of CPT-11, paclitaxel and other anticancer agents on human small cell lung cancer cells. *Cell Pharmacol.* 1996;3:1–6.
5. Yamada K, Ikehara M, Tanaka G, et al. Dose escalation study of paclitaxel in combination with fixed dose irinotecan in patients with advanced non-small cell lung cancer (JCOG9807). *Oncology.* 2004;66: 94–100.
6. Therasse P, Arbuck SG, Eisenhauer EA, et al. New guidelines to evaluate the response to treatment in solid tumors. *J Natl Cancer Inst.* 2000;92:205–216.
7. NCI-CTC, version 3, National Cancer Institute: Common Toxicity Criteria, version 2. http://ctep.cancer.gov/reporting/CTC-3.html.
8. Simon R. Optimal two-stage designs for phase II clinical trial. *Control Clin Trial.* 1989;10:1–10.
9. Schiller JH, Harrington D, Belani CP, et al. Comparison of four chemotherapy regimens for advanced non-small-cell lung cancer. *N Engl J Med.* 2002;346:92–98.
10. Yamamoto N, Negoro S, Chikazawa H, et al. Pharmacokinetic interaction of the combination of paclitaxel and irinotecan in vivo and clinical study [Abstract]. *Proc Am Soc Clin Oncol.* 1999;18:187.
11. Komuro Y, Udagawa Y, Susumu N, et al. Paclitaxel and SN-38 overcome cisplatin resistance of ovarian cancer cell lines by down-regulating the influx and efflux system of cisplatin. *Jpn J Cancer Res.* 2001;92: 1242–1250.

Distinctive Evaluation of Nonmucinous and Mucinous Subtypes of Bronchioloalveolar Carcinomas in *EGFR* and K-*ras* Gene-Mutation Analyses for Japanese Lung Adenocarcinomas

Confirmation of the Correlations With Histologic Subtypes and Gene Mutations

Yuji Sakuma, MD, PhD,[1] Shoichi Matsukuma, PhD,[1] Mitsuyo Yoshihara,[1] Yoshiyasu Nakamura,[1] Kazumasa Noda, MD, PhD,[2] Haruhiko Nakayama, MD, PhD,[2] Yoichi Kameda, MD, PhD,[3] Eiju Tsuchiya, MD, PhD,[1] and Yohei Miyagi, MD, PhD[1,4]

Key Words: Lung; Adenocarcinoma; Bronchioloalveolar; EGFR; K-ras; Mutation; Loop-hybrid mobility shift assay

DOI: 10.1309/WVXFGAFLAUX48DU6

Abstract

*Although adenocarcinomas of the lung are associated with epidermal growth factor receptor (*EGFR*) gene mutations and sensitivity to EGFR tyrosine kinase inhibitors, it remains unclear whether bronchioloalveolar carcinoma (BAC) components and/or subtypes affect these associations. We aimed to clarify correlations between* EGFR *gene mutations and BAC components and to establish the histologic features as reliable predictors for the mutations. We examined 141 non–small cell lung cancers (NSCLCs), including 118 adenocarcinomas, for mutations in exons 19 and 21 of the* EGFR *gene together with mutations in codon 12 of the K-*ras *gene using loop-hybrid mobility shift assays, a highly sensitive polymerase chain reaction–based method. Adenocarcinomas were subdivided into subtypes with a nonmucinous or mucinous BAC component and those without BAC components.*

In NSCLCs, EGFR *mutations were detected in 75 cases (53.2%) and were significantly associated with adenocarcinoma, female sex, and never smoking. Among adenocarcinomas, nonmucinous and mucinous BAC components were significantly associated with* EGFR *and K-*ras *gene mutations, respectively. Because* EGFR *mutations were detected even in most pure nonmucinous BACs, ie, lung adenocarcinoma in situ,* EGFR *mutation is considered a critical event in the pathogenesis of nonmucinous BAC tumors.*

In non–small cell lung cancers (NSCLCs), activating mutations in the tyrosine kinase domain of the epidermal growth factor receptor (*EGFR*) gene have been reported to be associated with sensitivity to EGFR tyrosine kinase inhibitors (TKIs), such as gefitinib and erlotinib. Furthermore, *EGFR* mutations are more frequently observed in patients with adenocarcinoma, people who have never smoked, women, and Asian patients.[1-10] These findings greatly mirror the increased response rates to EGFR TKIs in these groups of patients with NSCLCs.[11] In vitro experiments revealed that an NSCLC cell line with an *EGFR* mutation was 50-fold more sensitive to growth inhibition by gefitinib than cell lines with wild-type *EGFR*. In addition, autophosphorylation (activation) of EGFR was completely inhibited in the presence of a 100-fold smaller concentration of gefitinib than that required to inhibit wild-type EGFR.[2]

In the revised World Health Organization classification of 1999,[12] bronchioloalveolar carcinoma (BAC) is defined as "an adenocarcinoma with a pure lepidic growth pattern and no evidence of stromal, vascular or pleural invasion and subdivided into nonmucinous, mucinous or mixed type." Formerly, however, BAC cases were subclassified into mucinous, nonmucinous, and sclerotic subtypes, and a subset of the sclerotic type of BACs included clearly focally invasive adenocarcinomas with a lepidic growth pattern.[13,14] Because according to the 1999 World Health Organization classification most lung adenocarcinomas with a BAC component are now classified as adenocarcinoma, mixed subtype, the classification of BACs of the lung has remained controversial. The reported correlation between BAC histologic features and response to gefitinib is also controversial owing to the terminology. Miller et al[15] reported that a good response to gefitinib was more frequently

found in patients with "adenocarcinoma of the bronchioloalveolar subtype." Subsequently, several reports showed that adenocarcinomas with a BAC component were significantly correlated with *EGFR* mutations,[1,3,16-18] although other studies did not confirm the correlation.[6,8,9]

Mutations in K-*ras*, a known downstream signaling molecule in the EGFR signaling pathway, have been detected in a subset of lung adenocarcinomas. Interestingly, most mucinous subtypes of BAC have been reported to harbor K-*ras* mutations.[14,19] Although nonmucinous and mucinous subtypes of BACs are clinically, biologically, and histologically distinct from one another,[14] most[1-4,6-10,15-17] (except a few[5,18]) reports have not subdivided the BACs into nonmucinous and mucinous subtypes, and, therefore, relationships between BAC subtypes and *EGFR* and K-*ras* gene mutations have remained unclear.

Since we previously developed a rapid, easy, and sensitive method for detecting known point mutations and deletion mutations,[20] we examined NSCLC specimens from Japan for mutations in *EGFR* exons 19 and 21 and K-*ras* codon 12 and analyzed the relationships between the *EGFR* or K-*ras* gene mutational status and clinicopathologic features, especially histopathologic features, to clarify the roles of *EGFR* and K-*ras* mutations in the pathogenesis of NSCLCs, especially adenocarcinomas. In addition, we examined adenocarcinoma specimens for expression and phosphorylation status of EGFR and analyzed the association between *EGFR* gene mutations and the expression level or phosphorylation status of EGFR.

Materials and Methods

Cases and Tissue Specimens

Surgically resected specimens of 141 primary NSCLCs, consisting of 118 adenocarcinomas, 2 adenosquamous carcinomas, and 21 squamous cell carcinomas, were obtained from Kanagawa Cancer Center Hospital (Yokohama, Japan) during the period from January 2002 to August 2004. Institutional review board permission and informed consent were obtained for all cases.

BAC was defined as an adenocarcinoma with a pure lepidic growth pattern and no evidence of stromal, vascular, or plural invasion, ie, a peripheral lung adenocarcinoma in situ.[12] In nonmucinous subtypes, the neoplastic cells are cuboidal and usually show apical snouts and a hobnailed appearance. In mucinous subtypes, alveolar walls are lined by a cellular proliferation of columnar cells with abundant apical mucin and small basally oriented nuclei.[12] Small peripheral lung adenocarcinomas are subdivided as follows: (1) with a BAC component (replacing growth type), which are further subdivided into pure BAC and mixed BAC and invasive components, and (2) without BAC components (nonreplacing and destructive growth type).[21]

In this study, all pathology slides of the 118 adenocarcinomas were reviewed and reclassified as follows: (1) adenocarcinoma with a nonmucinous BAC component (n = 82), including pure nonmucinous BAC (n = 17) and invasive adenocarcinoma with a nonmucinous BAC component (n = 65); (2) adenocarcinoma without BAC components (n = 27); and (3) adenocarcinoma with a mucinous BAC component (n = 9), including pure mucinous BAC (n = 2) and invasive adenocarcinoma with a mucinous BAC component (n = 7). These diagnoses were independently made by 3 pathologists (Y.S., Y.K., and E.T.). Discrepancies in diagnoses were resolved by mutual agreement. The 141 patients with NSCLC included 69 men and 72 women with a median age of 65 years (range, 39-86 years). The 118 patients with adenocarcinoma included 51 men and 67 women with a median age of 64 years (range, 39-86 years). In total, 105 patients had stage I disease, 13 had stage II, 22 had stage III, and 1 had stage IV. There were 64 patients who had never smoked and 77 who had, including 35 current and 42 former smokers.

Immunohistochemical Studies for EGFR and Phospho-EGFR

Formalin-fixed, paraffin-embedded tissue sections of the 118 adenocarcinomas were prepared. The level of EGFR expression was determined by immunohistochemical analysis using an EGFR PharmDx kit (k1492; DAKO Japan, Kyoto, Japan), according to the manufacturer's recommendations. Each slide was scored as positive if more than 5% of tumor cells had membranous staining. The membranous staining intensity was evaluated using a 0 to 3+ scale, in which scores of 0 or 1+ were considered negative for EGFR overexpression and scores of 2+ or 3+ were positive. The presence or absence of phosphorylated EGFR (phospho-EGFR) expression was determined by immunohistochemical analysis using a mouse monoclonal antibody, pY1173EGFR (K1497; kindly provided by DAKO Japan), which specifically recognizes phosphorylated tyrosine at codon 1173 of EGFR, according to the manufacturer's protocol. Each slide was considered positive if more than 5% of tumor cells exhibited membranous staining but negative if the staining was only cytoplasmic.

DNA Preparations and Plasmid Clones

Formalin-fixed, paraffin-embedded tissue sections were used for DNA isolation from the tumor tissues. Briefly, a drop of pinpoint solution (Pinpoint Slide DNA Isolation System; Zymo Research, Orange, CA) was applied to the exact area of the tumor, of approximately 5 × 5 mm^2, which was identified in H&E-stained serial sections, and DNA was extracted according to the manufacturer's instructions. Cloning of polymerase chain reaction (PCR) products into plasmids was carried out

DOI: 10.1309/WVXFGAFLAUX48DU6

using the TOPO-TA ligation vector, pCR4TOPO (Invitrogen, Carlsbad, CA). The cloned plasmids were amplified with Phi29 polymerase (Amersham Bioscience, Piscataway, NJ) and used for sequencing of the inserted tumor DNA fragments (CEQ8000 Sequence Analysis System, Beckman Coulter, Fullerton, CA).

Loop-Hybrid Mobility Shift Assay

The loop-hybrid mobility shift assay (LH-MSA)[20] consisted of 2 parts: (1) hybridization of PCR products with loop-hybrid generator (LH-G) probes of synthetic oligonucleotides (75mer to 99mer) to generate loop hybrids and (2) detection of retarded-mobility bands of the loop hybrids in native polyacrylamide gel electrophoresis. The nucleotide sequences of the PCR primers and LH-G probes used to detect hot spot point mutations (E7R for *EGFR* exon 21 at L858; K7F for K-*ras* exon 2 at G12) and deletion mutations (19JWTF for *EGFR* exon 19) in the present study are described in ▮Table 1▮.

PCR was performed with Accuprime *Taq* polymerase together with primer-template hybridization enhancing reagent (Invitrogen). Generation of loop hybrids was carried out at the end of the PCR amplification cycles by adding a specific LH-G probe into the PCR reaction solution to a final concentration of 500 nmol/L. The mixture was then treated by the loop-hybrid formation steps consisting of denaturation at 94°C for 2 minutes, hybridization of the LH-G probe to the complementary strand at 55°C for 15 seconds, and extension of the 3' end of the LH-G probe in loop hybrids by *Taq* polymerase at 68°C for 4 minutes. The reaction products after the loop-hybrid formation steps were subjected to polyacrylamide gel electrophoresis for detection of mobility-shifted loop-hybrid bands by mutations. The gels were stained with SYBER Green I (Cambrex Bio Science, Rockland, ME), and the DNA bands were detected with the laser scanning imager (STORM 860, GE Healthcare Biosciences, Piscataway, NJ). The DNA bands with mutations detected by the LH-MSA were cloned into plasmids and sequenced.

Statistical Analyses

We looked for associations between *EGFR* or K-*ras* mutations and various patient characteristics, including age, sex, smoking history, stage of disease, pathologic subtype, EGFR overexpression, and phospho-EGFR expression. The χ^2 test or Fisher exact test was conducted to analyze the associations between mutations and each of the potentially influential factors. The Fisher exact test was performed if there were 5 or fewer observations in a group. The Mann-Whitney *U* test was used to assess the relationships between *EGFR* mutations and the expression level of EGFR. To identify which independent factors had a significant influence on the incidence of *EGFR* or K-*ras* mutations, logistic regression models were used. Probability values of less than .05 were defined as statistically significant.

Results

EGFR Mutations in NSCLCs

▮Table 2▮ summarizes a total of 88 *EGFR* mutations among 75 NSCLCs detected in this study. *EGFR* mutations were detected in 75 (53.2%) of 141 patients with NSCLC ▮Image 1▮. Among the 75 patients with *EGFR* mutations, 13 (17%) had multiple mutations. We found that 40 (53%) had in-frame deletion mutations in exon 19, 26 (35%) had a point mutation in exon 21, and 9 (12%) had deletion and point mutations in exons 19 and 21, respectively. Among the 40 patients with deletion mutations, of whom 4 had double mutations, all 44 mutations occurred around codons 747 to 749 in exon 19. Among the 26 patients with a point mutation in exon 21, 24 had an L858R mutation. In the 9 patients with both exon 19 deletion and exon 21 point mutations, all 9 of the 9 deletion mutations and most (8/9 [89%]) of the point mutations occurred around codons 747 to 749 and at codon 858, respectively.

▮Table 1▮
PCR Primers and LH-G Probes Used for Detection of Mutations in *EGFR* and K-*ras*

Gene	Mutation	Amplicon (bp)	PCR Primer	LH-G Probe† (Probe Name)
EGFR	In-frame deletion in exon 19	212	F: GGACTCTGGATCCCAGAAGGTG; R: CATTTAGGATGTGGAGATGAGC	GGACTCTGGA TCCCAGAAGG TGAGAAAGTT AAAATTCCCG TCGCTATCAA GGAATTAAGA GAAGCAACAT CTCCGAAAGC CAACAAGGAA ATCCTCGAT (19JWTF)
EGFR	Point mutation in exon 21 at L858	161	F: GGCATGAACTACTTGGAGGAC; R: CTTACTTTGCCTCCTTCTGCATG	CTTACTTTGC CTCCTTCTGC ATGGTATTCT TTCTCTTCCG CACCCAGCAG *******AGC CCAAAATCTG TGATCTTGAC ATGCTGCG (E7R)
K-*ras*	Point mutation in exon 2 at G12	165	F: AAGGCCTGCTGAAAATGACTG; R: GGTCCTGCACCAGTAATATGCA	AAGGCCTGCT GAAAATGACT GAATATAAAC TTGTGGTAGT TGGAGCTGG* ******GGCA AGAGTGCCTT GACGATACAG CT (K7F)

bp, base pairs; EGFR, epidermal growth factor receptor; F, forward; LH-G, loop-hybrid generator; PCR, polymerase chain reaction; R, reverse.
†Asterisks indicate deleted nucleotides; underlined type, nucleotides for the hot spots of mutations to be detected.

DOI: 10.1309/WVXFGAFLAUX48DU6

Table 2
Summary of 88 Mutations Detected in the Tyrosine Kinase Domain of the *EGFR* Gene

Type of Mutation	Exon	Nucleotide Change	Amino Acid Change	No. of Cases
In-frame deletion	19	del2235-2249	del746-750	14
		del2239-2247, G2248>C	del747-749, A750P	9
		del2236-2250	del746-750	5
		del2240-2254	del747-751	4
		del2237-2254, C2255>T	E746V, del747-752	2
		del2239-2256	del747-752	1
		del2240-2257	L747S, del748-753	1
		del2235-2249 and del2239-2247, G2248>C	del746-750 and del747-749, A750P	2
		del2239-2247, G2248>C and del2236-2250	del747-749, A750P and del746-750	1
		del2239-2247, G2248>C and del2240-2254	del747-749, A750P and del747-751	1
Single-nucleotide substitution	21	T2573>G	L858R	24
		G2575>A	A859T	1
		T2582>G	L861R	1
In-frame deletion and single-nucleotide substitution	19 and 21	del2239-2247, G2248>C and T2573>G	del747-749, A750P and L858R	5
		del2235-2249 and T2573>G	del746-750 and L858R	2
		del2235-2249 and T2582>G	del746-750 and L861R	1
		del2236-2250 and T2573>G	del746-750 and L858R	1

EGFR, epidermal growth factor receptor.

Relationships Between *EGFR* Mutations and Clinicopathologic Features

We analyzed the relationships between the *EGFR* gene status and clinicopathologic factors **Table 3**. *EGFR* mutations were significantly more frequent in women than in men, in never-smokers than in ever-smokers, and in patients with adenocarcinomas than in patients with nonadenocarcinomas (1/23 [4%]) among the 141 NSCLCs. No statistically significant associations were found between the *EGFR* mutation status and age or tumor stage (Table 3). Logistic regression models suggested that adenocarcinoma histologic features ($P = .0047$) and female sex ($P = .0084$) independently affected the incidence of *EGFR* mutations, whereas smoking status ($P = .2385$) did not.

Because adenocarcinoma was the dominant histologic diagnosis for *EGFR* mutations, further analyses were limited to adenocarcinomas. *EGFR* mutations were significantly associated with older age at diagnosis, female sex, never smoking, and histologic features with a nonmucinous BAC component, including pure nonmucinous BACs and invasive adenocarcinoma with a nonmucinous BAC component, compared with younger age at diagnosis, male sex, ever smoking, and a histologic diagnosis other than a nonmucinous BAC subtype (10/36 [28%]), respectively. There was no significant relationship between *EGFR* mutations and tumor stage (Table 3). Logistic regression models showed that a nonmucinous BAC component ($P = .0006$) and female sex ($P = .0083$) were independent variables, whereas smoking status ($P = .9105$) and age at diagnosis ($P = .3083$) were not **Image 2A**.

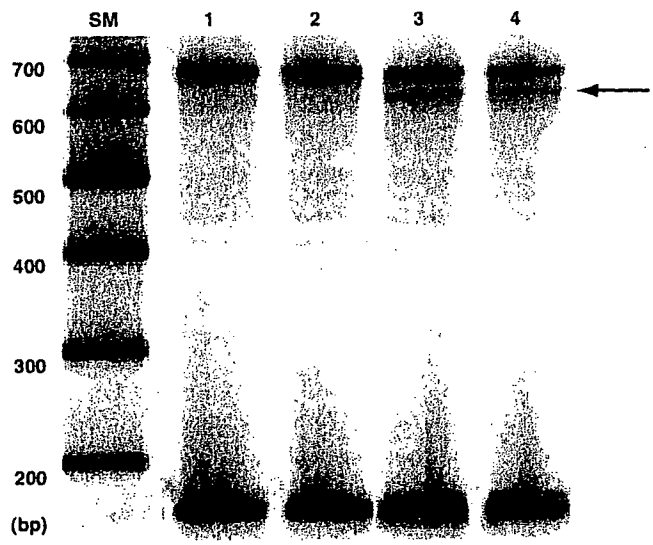

Image 1 Detection of point mutations at codon 858 of the epidermal growth factor receptor gene exon 21. The electrophoretogram after loop-hybrid mobility shift assay to detect the point mutation L858R in the tumor DNA in lung adenocarcinomas. Lanes 1 and 2 show normal sequences; lanes 3 and 4, heterozygous mutations; arrow, mutational bands. The homoduplex bands are at 161 bp. bp, base pair; SM, size marker.

Expression of EGFR and Phospho-EGFR

Table 4 summarizes the relationships between *EGFR* mutations and EGFR expression among the 118 adenocarcinomas studied. There was no statistically significant difference between *EGFR* mutations and the intensity of EGFR expression ($P = .1799$). When scores of 0 or 1+ were considered negative for EGFR overexpression and scores of 2+ or 3+ were considered positive, no statistically significant association between *EGFR* mutations and EGFR overexpression was found (Table 3; $P = .0631$). Phospho-EGFR expression was observed in 21

DOI: 10.1309/WVXFGAFLAUX48DU6

Table 3
Patient Characteristics and Frequency of *EGFR* Mutations

Variable	No. of Cases	No. (%) of *EGFR* Mutations	*P*
NSCLC (n = 141)			
Age (y)			NS
≤65	73	36 (49)	
>65	68	39 (57)	
Sex			<.0001
Male	69	21 (30)	
Female	72	54 (75)	
Smoking history			<.0001
Never smoked	64	50 (78)	
Ever smoked	77	25 (32)	
Histologic diagnosis			<.0001*
Adenocarcinoma	118	74 (62.7)	
Adenosquamous carcinoma	2	0 (0)	
Squamous cell carcinoma	21	1 (5)	
Stage			NS
IA and IB	105	59 (56.2)	
II through IV	36	16 (44)	
Adenocarcinoma (n = 118)			
Age (y)			.0321
≤64	60	32 (53)	
>64	58	42 (72)	
Sex			<.0001
Male	51	20 (39)	
Female	67	54 (81)	
Smoking history			.0002
Never smoked	64	50 (78)	
Ever smoked	54	24 (44)	
Histologic diagnosis			<.0001†
Adenocarcinoma with a nonmucinous BAC component‡	82	64 (78)	
Adenocarcinoma without BAC components	27	8 (30)	
Adenocarcinoma with a mucinous BAC component	9	2 (22)	
Stage			NS
IA and IB	93	59 (63)	
II through IV	25	15 (60)	
Overexpression of EGFR			NS
Positive	54	29 (54)	
Negative	64	45 (70)	
Expression of phospho-EGFR			NS
Positive	21	17 (81)	
Negative	97	57 (59)	

BAC, bronchioloalveolar carcinoma; EGFR, epidermal growth factor receptor; NS, not significant; NSCLC, non–small cell lung cancer; phospho-EGFR, phosphorylated EGFR.
* Histologic differences were examined between adenocarcinoma and other types of NSCLCs in 141 NSCLCs.
† Histologic differences were examined between adenocarcinoma with a nonmucinous BAC component and other subtypes of adenocarcinomas in 118 adenocarcinomas.
‡ Adenocarcinoma with a nonmucinous BAC component included pure nonmucinous BAC (15/17 [88%]) and invasive adenocarcinoma with a nonmucinous BAC component (49/65 [75%]).

(17.8%) of 118 adenocarcinomas studied. No statistically significant association between *EGFR* mutations and expression of phospho-EGFR was observed (Table 3; $P = .0806$).

Relationships Between K-*ras* Mutations and Clinicopathologic Features

K-*ras* mutations at codon 12 were present in 10 (8.5%) of 118 adenocarcinomas but not in the other histologic types (0 of 23) examined. The mutations consisted of six 34G>T (G12C), two 35G>A (G12D), and single examples of 35G>C (G12A) and 35G>T (G12V). K-*ras* mutations were significantly more frequent in ever-smokers than in never-smokers, in tumors with histologic features with a mucinous BAC component than in those without a mucinous BAC component (4/109 [3.7%]), and in tumors with the wild-type *EGFR* gene than tumors with mutated *EGFR* among the 118 adenocarcinomas. Neither age at diagnosis nor sex significantly modified the frequency of K-*ras* mutations **Table 5**. Logistic regression analyses demonstrated that a mucinous BAC component ($P = .0002$) was the only significant determinant for K-*ras* mutations, whereas smoking history ($P = .0699$) and *EGFR* mutation status ($P = .1648$) were not **Image 2B**.

EGFR and K-*ras* Mutations in Nonmucinous and Mucinous BAC Subtypes

To date, only 3 studies, including the present study and 2 previous reports,[5,18] subdivided BACs into nonmucinous and mucinous subtypes and examined them for *EGFR* and K-*ras*

DOI: 10.1309/WVXFGAFLAUX48DU6

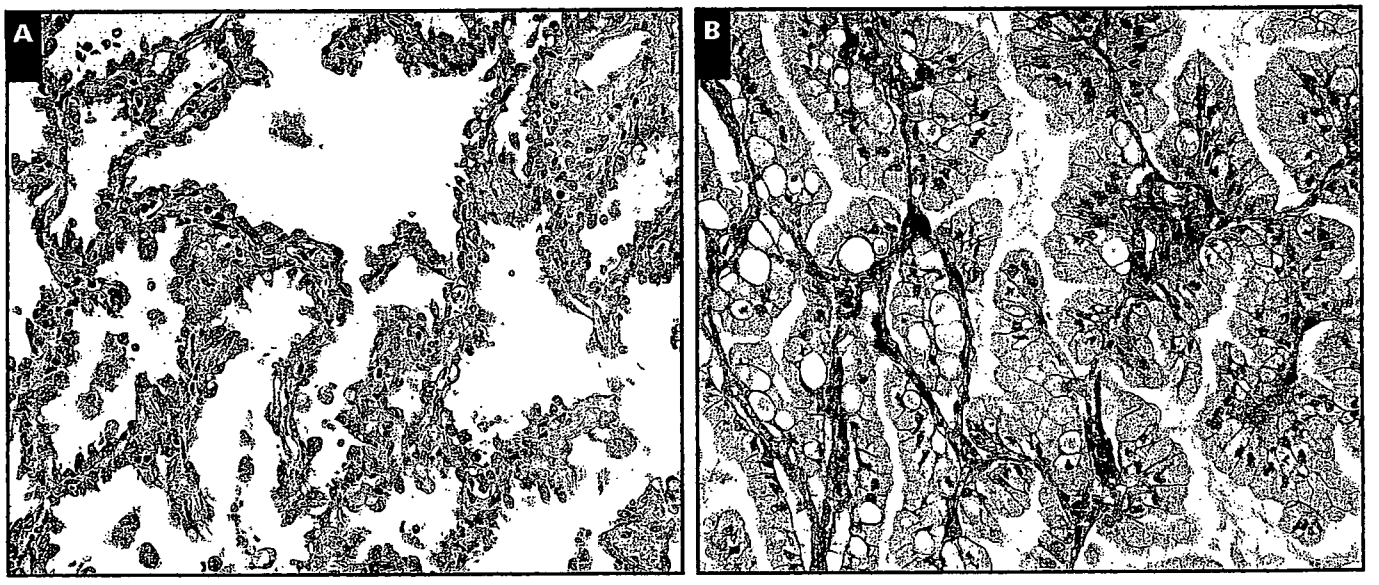

Image 2 Typical histopathologic features of epidermal growth factor receptor (*EGFR*)- and K-*ras*–mutated lung adenocarcinomas. **A**, Nonmucinous bronchioloalveolar carcinoma (BAC) component of an *EGFR*-mutated adenocarcinoma. This tumor has a deletion mutation (del746-750) in exon 19. **B**, Mucinous BAC component of a K-*ras*–mutated adenocarcinoma. This tumor harbors a point mutation (G12V).

mutations. **Table 6** shows a summary of *EGFR* and K-*ras* gene mutational frequencies in the 2 BAC subtypes studied.

Discussion

We have shown that adenocarcinomas with a nonmucinous or mucinous BAC component are significantly associated with *EGFR* or K-*ras* gene mutations, respectively. Some previous reports did not distinguish nonmucinous and mucinous BAC subtypes and did not confirm a significant association between histologic features with a BAC component and

Table 4
Relationship Between *EGFR* Mutations and EGFR Expression in 118 Adenocarcinomas

	EGFR Expression			
***EGFR* Mutation**	**0**	**1+**	**2+**	**3+**
Positive (n = 74)	25	20	11	18
Negative (n = 44)	12	7	12	13

Table 5
Characteristics and Frequency of K-*ras* Mutations in 118 Patients With Adenocarcinoma

Variable	No. of Cases	No. (%) of K-*ras* Mutations	*P*
Age (y)			NS
≤64	60	3 (5)	
>64	58	7 (12)	
Sex			NS
Male	51	7 (14)	
Female	67	3 (4)	
Smoking history			.0053
Never smoked	64	1 (2)	
Ever smoked	54	9 (17)	
Histologic diagnosis			<.0001*
Adenocarcinoma with a nonmucinous BAC component†	82	2 (2)	
Adenocarcinoma without BAC components	27	2 (7)	
Adenocarcinoma with a mucinous BAC component	9	6 (67)	
EGFR mutation			.0055
Mutated	74	2 (3)	
Wild-type	44	8 (18)	

BAC, bronchioloalveolar carcinoma; EGFR, epidermal growth factor receptor; NS, not significant.
* The histologic difference was analyzed between adenocarcinoma with a mucinous BAC component and other subtypes of adenocarcinomas.
† Adenocarcinomas with a nonmucinous BAC component included pure nonmucinous BAC (1/17 [6%]) and invasive adenocarcinoma with a nonmucinous BAC component (1/65 [2%]).

DOI: 10.1309/WVXFGAFLAUX48DU6

EGFR mutations.[6,8,9] Our present results clearly demonstrate that BAC histologic features should be further distinctively considered as nonmucinous and mucinous subtypes.

Our present findings, demonstrating mutually exclusive *EGFR* and K-*ras* gene mutations in nonmucinous and mucinous BACs, respectively, totally agree with a previous report by Marchetti et al[5] in Italy on this point, but a significant difference exists. Comparing these 2 studies reveals that the frequency of *EGFR* mutations in pure nonmucinous BACs, ie, peripheral lung adenocarcinomas in situ, was quite different (Table 6). We found 88% *EGFR* mutations in pure nonmucinous BACs, and Marchetti et al[5] reported a frequency of 32%. In addition, a more recent report from Hong Kong demonstrated that 15 (79%) of 19 nonmucinous BAC-type tumors had *EGFR* mutations, although these tumors included pure BACs and focally invasive tumors (Table 6).[18]

Because previous reports clarified that the frequency of *EGFR* mutations in lung adenocarcinomas, including all histologic subtypes in East Asia, was much higher than that in other areas, such as the United States, Italy, and Australia,[1-10] one could speculate that the difference of *EGFR* mutational prevalence, even in a specific histologic subtype, ie, pure nonmucinous BAC, comes from the genetic differences of racial background between East Asians and Italians. Of course, there might be differences of interpretation of diagnostic criteria for nonmucinous BAC by pathologists from different countries, and further studies are needed to clarify the incidence of *EGFR* mutations in pure nonmucinous BACs, especially in areas other than East Asia.

Pure nonmucinous BACs are thought to sequentially progress to invasive adenocarcinomas with a nonmucinous BAC component from the point of clinicopathologic and molecular evidence.[21-23] In the present study, the frequency (49/65 [75%]) of *EGFR* mutations in invasive adenocarcinomas with a nonmucinous BAC component was almost the same as that (15/17 [88%]) in pure nonmucinous BACs. Our results were obtained from simultaneous analyses in 1 institute with the same method and, therefore, strongly support the view of sequential progression from nonmucinous BACs to invasive adenocarcinomas with a nonmucinous BAC component from the *EGFR* gene alteration aspect.

Our results of *EGFR* gene mutation analyses generally confirmed the results obtained in previous studies in relation to the incidence in NSCLCs, by sex, and by smoking status.[1-10] We also demonstrated that 9 (12%) of 75 NSCLCs with *EGFR* mutations had mutations in exons 19 and 21 (Table 2), of which 3 were pure nonmucinous BACs and the others were invasive adenocarcinomas with a nonmucinous BAC component. In addition, 4 (5%) of 75 tumors (3 adenocarcinomas with a nonmucinous BAC component and 1 pure mucinous BAC) had 2 distinct deletion mutations in exon 19. Identical double mutations in exons 19 and 21 of the *EGFR* gene have also been reported in 1 of 28 NSCLC tissues with *EGFR* mutations[9] and in 3 of 19 *EGFR*-mutated NSCLC cell lines.[24] Because all double *EGFR* mutations in the present study and others[9,24] occurred de novo without prior treatments, the *EGFR* gene might be prone to be targeted in a subset of NSCLCs.

Table 6
Summary of *EGFR* and K-*ras* Mutations in BAC Subtypes*

BAC Subtype	No. of Cases	*EGFR* Mutation	K-*ras* Mutation
Marchetti et al[5]			
Nonmucinous	69	22 (32)	10 (14)
Mucinous	17	0 (0)	13 (76)
Tam et al[18†]			
Nonmucinous	19	15 (79)	NA
Mucinous	5	0 (0)	NA
Present study			
Nonmucinous	17	15 (88)	1 (6)
Mucinous‡	9	2 (22)	6 (67)

BAC, bronchioloalveolar carcinoma; EGFR, epidermal growth factor receptor; NA, not available.
* Data are given as number (percentage).
† Tam et al[18] subdivided 215 adenocarcinomas into non–BAC-type (n = 191) and BAC-type (n = 24) tumors. They mentioned that 17 of 24 BAC-type adenocarcinomas did not show invasive growth.
‡ The present study includes 2 pure mucinous BACs and 7 focally invasive adenocarcinomas with a predominant mucinous BAC component.

K-*ras* mutations were detected only in adenocarcinomas and were significantly associated with ever smoking, tumors with the wild-type *EGFR* gene, and histologic features with a mucinous BAC component. These results are consistent with those in previous reports.[6,14,18,19] The *EGFR* and K-*ras* gene mutations were generally mutually exclusive of each other in lung adenocarcinomas in the present and reported studies.[4-6,18,25-27] To the best of our knowledge, only 4 lung adenocarcinomas with hot spot mutations in both the *EGFR* and K-*ras* genes have been reported, but histologic characteristics of these tumors were not mentioned.[28,29] Interestingly, Han et al[29] reported that neither of 2 patients with double mutations in *EGFR* and K-*ras* genes responded to gefitinib despite having a gefitinib-sensitive *EGFR* mutation (G719A or deletion in exon 19). In the present study, 2 adenocarcinomas with double mutations had mucinous but not nonmucinous BAC components. Considering these facts, from response to EGFR TKI and morphologic phenotypes, adenocarcinomas with double mutations in *EGFR* and K-*ras* genes might show the same characteristics as K-*ras*–mutated adenocarcinoma but not *EGFR*-mutated adenocarcinoma.

We studied NSCLC tissue samples for mutations of the *EGFR* and K-*ras* genes using LH-MSA technique,[20] which was previously developed by one of us (S.M.). The LH-MSA technique is considered a sensitive and specific, rapid, simple PCR-based method, although in principle, it can only apply to detecting known hot spot mutations. We consider that the high sensitivity and specificity of LH-MSA could be a powerful

DOI: 10.1309/WVXFGAFLAUX48DU6

tool for further elucidating the clinicopathologic characteristics of *EGFR*- and K-*ras*–mutated lung adenocarcinomas.

Amplification of the *EGFR* gene has been reported to be an effective molecular predictor for EGFR TKIs efficacy,[30] although curiously, the presence or intensity of EGFR protein expression in pathologic specimens determined by immunohistochemical analysis has been considered not a predictor.[31] We surmised that the phosphorylation (activation) status rather than the expression intensity of EGFR is a good predictor for sensitivity to EGFR TKIs. Although 17 (81%) of 21 adenocarcinomas with phospho-EGFR expression had *EGFR* gene mutations, no statistically significant association between *EGFR* mutations and expression of phospho-EGFR determined by immunohistochemical analysis was observed. Furthermore, no statistically significant association between *EGFR* mutations and overexpression of the protein was confirmed.

We have demonstrated that lung adenocarcinomas with a nonmucinous or mucinous BAC component are significantly correlated with *EGFR* or K-*ras* mutations, respectively. Together with other published studies,[1-5,15,18] our finding that most pure nonmucinous BACs already have *EGFR* mutations leads us to believe that the *EGFR* gene is an addicted oncogene in the pathogenesis of nonmucinous BAC-type lung adenocarcinomas but not mucinous BAC-type tumors. Further clarification of the molecular mechanisms responsible for the progression from nonmucinous BACs to invasive adenocarcinomas should provide new therapeutic targets in addition to EGFR.

From the [1]Molecular Pathology and Genetics Division, Kanagawa Cancer Center Research Institute, and the Departments of [2]Thoracic Oncology and [3]Pathology and [4]Laboratory for Molecular Diagnostics, Kanagawa Cancer Center Hospital, Yokohama, Japan.

Supported in part by the Kanagawa Cancer Research Fund and the Smoking Research Foundation, Tokyo, Japan (Y.M.).

Address reprint requests to Dr Miyagi: Molecular Pathology and Genetics Division, Kanagawa Cancer Center Research Institute, Nakao 1-1-2, Asahi-ku, Yokohama 241-0815, Japan.

References

1. Lynch TJ, Bell DW, Sordella R, et al. Activating mutations in the epidermal growth factor receptor underlying responsiveness of non–small-cell lung cancer to gefitinib. *N Engl J Med.* 2004;350:2129-2139.
2. Paez JG, Janne PA, Lee JC, et al. *EGFR* mutations in lung cancer: correlation with clinical response to gefitinib therapy. *Science.* 2004;304:1497-1500.
3. Pao W, Miller V, Zakowski M, et al. EGF receptor gene mutations are common in lung cancers from "never smokers" and are associated with sensitivity of tumors to gefitinib and erlotinib. *Proc Natl Acad Sci U S A.* 2004;101:13306-13311.
4. Kosaka T, Yatabe Y, Endoh H, et al. Mutations of the epidermal growth factor receptor gene in lung cancer: biological and clinical implications. *Cancer Res.* 2004;64:8919-8923.
5. Marchetti A, Martella C, Felicioni L, et al. *EGFR* mutations in non–small-cell lung cancer: analysis of a large series of cases and development of a rapid and sensitive method for diagnostic screening with potential implications on pharmacologic treatment. *J Clin Oncol.* 2005;23:857-865.
6. Shigematsu H, Lin L, Takahashi T, et al. Clinical and biological features associated with epidermal growth factor receptor gene mutations in lung cancers. *J Natl Cancer Inst.* 2005;97:339-346.
7. Tokumo M, Toyooka S, Kiura K, et al. The relationship between epidermal growth factor receptor mutations and clinicopathologic features in non–small cell lung cancers. *Clin Cancer Res.* 2005;11:1167-1173.
8. Chou TY, Chiu CH, Li LH, et al. Mutation in the tyrosine kinase domain of epidermal growth factor receptor is a predictive and prognostic factor for gefitinib treatment in patients with non–small cell lung cancer. *Clin Cancer Res.* 2005;11:3750-3757.
9. Mu XL, Li LY, Zhang XT, et al. Gefitinib-sensitive mutations of the epidermal growth factor receptor tyrosine kinase domain in Chinese patients with non–small cell lung cancer. *Clin Cancer Res.* 2005;11:4289-4294.
10. Sonobe M, Manabe T, Wada H, et al. Mutations in the epidermal growth factor receptor gene are linked to smoking-independent, lung adenocarcinoma. *Br J Cancer.* 2005;93:355-363.
11. Janne PA, Engelman JA, Johnson BE. Epidermal growth factor receptor mutations in non–small-cell lung cancer: implications for treatment and tumor biology. *J Clin Oncol.* 2005;23:3227-3234.
12. Travis W, Colby T, Corrin B, et al. *Histological Typing of Lung and Pleural Tumors.* Berlin, Germany: Springer; 1999:28-40. *World Health Organization International Histological Classification of Tumours.*
13. Barsky SH, Cameron R, Osann KE, et al. Rising incidence of bronchioloalveolar lung carcinoma and its unique clinicopathologic features. *Cancer.* 1994;73:1163-1170.
14. Marchetti A, Buttitta F, Pellegrini S, et al. Bronchioloalveolar lung carcinomas: K-*ras* mutations are constant events in the mucinous subtype. *J Pathol.* 1996;179:254-259.
15. Miller VA, Kris MG, Shah N, et al. Bronchioloalveolar pathologic subtype and smoking history predict sensitivity to gefitinib in advanced non–small-cell lung cancer. *J Clin Oncol.* 2004;22:1103-1109.
16. Yatabe Y, Kosaka T, Takahashi T, et al. *EGFR* mutation is specific for terminal respiratory unit type adenocarcinoma. *Am J Surg Pathol.* 2005;29:633-639.
17. Haneda H, Sasaki H, Shimizu S, et al. Epidermal growth factor receptor gene mutation defines distinct subsets among small adenocarcinomas of the lung. *Lung Cancer.* 2006;52:47-52.
18. Tam IY, Chung LP, Suen WS, et al. Distinct epidermal growth factor receptor and KRAS mutation patterns in non–small cell lung cancer patients with different tobacco exposure and clinicopathologic features. *Clin Cancer Res.* 2006;12:1647-1653.
19. Tsuchiya E, Furuta R, Wada N, et al. High K-*ras* mutation rates in goblet-cell-type adenocarcinomas of the lungs. *J Cancer Res Clin Oncol.* 1995;121:577-581.
20. Matsukuma S, Yoshihara M, Kasai F, et al. Rapid and simple detection of hot spot point mutations of epidermal growth factor receptor, BRAF, and *NRAS* in cancers using the loop-hybrid mobility shift assay. *J Mol Diagn.* 2006;8:504-512.
21. Noguchi M, Morikawa A, Kawasaki M, et al. Small adenocarcinoma of the lung: histologic characteristics and prognosis. *Cancer.* 1995;75:2844-2852.

DOI: 10.1309/WVXFGAFLAUX48DU6

22. Aoyagi Y, Yokose T, Minami Y, et al. Accumulation of losses of heterozygosity and multistep carcinogenesis in pulmonary adenocarcinoma. *Cancer Res*. 2001;61:7950-7954.
23. Koga T, Hashimoto S, Sugio K, et al. Clinicopathological and molecular evidence indicating the independence of bronchioloalveolar components from other subtypes of human peripheral lung adenocarcinoma. *Clin Cancer Res*. 2001;7:1730-1738.
24. Nagai Y, Miyazawa H, Huqun, et al. Genetic heterogeneity of the epidermal growth factor receptor in non–small cell lung cancer cell lines revealed by a rapid and sensitive detection system, the peptide nucleic acid-locked nucleic acid PCR clamp. *Cancer Res*. 2005;65:7276-7282.
25. Soung YH, Lee JW, Kim SY, et al. Mutational analysis of *EGFR* and K-*ras* genes in lung adenocarcinomas. *Virchows Arch*. 2005;446:483-488.
26. Shigematsu H, Gazdar AF. Somatic mutations of epidermal growth factor receptor signaling pathway in lung cancers. *Int J Cancer*. 2006;118:257-262.
27. Tsao AS, Tang X, Sabloff B, et al. Clinicopathologic characteristics of the *EGFR* gene mutation in non–small cell lung cancer. *J Thorac Oncol*. 2006;1:231-239.
28. Eberhard DA, Johnson BE, Amler LC, et al. Mutations in the epidermal growth factor receptor and in KRAS are predictive and prognostic indicators in patients with non–small-cell lung cancer treated with chemotherapy alone and in combination with erlotinib. *J Clin Oncol*. 2005;23:5900-5909.
29. Han SW, Kim TY, Jeon YK, et al. Optimization of patient selection for gefitinib in non–small cell lung cancer by combined analysis of epidermal growth factor receptor mutation, K-*ras* mutation, and Akt phosphorylation. *Clin Cancer Res*. 2006;12:2538-2544.
30. Cappuzzo F, Hirsch FR, Rossi E, et al. Epidermal growth factor receptor gene and protein and gefitinib sensitivity in non–small-cell lung cancer. *J Natl Cancer Inst*. 2005;97:643-655.
31. Shah NT, Kris MG, Pao W, et al. Practical management of patients with non–small-cell lung cancer treated with gefitinib. *J Clin Oncol*. 2005;23:165-174.

DOI: 10.1309/WVXFGAFLAUX48DU6

Oncogene (2007) 26, 4025–4031

www.nature.com/onc

SHORT COMMUNICATION

CLCP1 interacts with semaphorin 4B and regulates motility of lung cancer cells

H Nagai[1,2,3], N Sugito[2], H Matsubara[1,3], Y Tatematsu[2], T Hida[4], Y Sekido[2], M Nagino[3], Y Nimura[3], T Takahashi[1,2] and H Osada[2]

[1]Division of Molecular Carcinogenesis, Center for Neurological Diseases and Cancer, Nagoya University Graduate School of Medicine, Nagoya, Japan; [2]Division of Molecular Oncology, Aichi Cancer Center Research Institute, Nagoya, Japan; [3]Division of Surgical Oncology, Department of Surgery, Nagoya University Graduate School of Medicine, Nagoya, Japan and [4]Department of Pulmonary Medicine, Aichi Cancer Center Hospital, Nagoya, Japan

We previously established a highly metastatic subline, LNM35, from the NCI-H460 lung cancer cell line, and demonstrated upregulation of a novel gene, *CLCP1* (CUB, LCCL-homology, coagulation factor V/VIII homology domains protein), in LNM35 and lung cancer specimens. In this study, we focused on the potential roles of that gene in cancer metastasis. First, we established stable LNM35 RNAi clones, in which *CLCP1* expression was suppressed by RNAi, and found that their motility was significantly reduced, although growth rates were not changed. Next, *in vitro* selection of a phage display library demonstrated that a phage clone displaying a peptide similar to a sequence within the Sema domain of semaphorin 4B (SEMA4B) interacted with LNM35. Immunoprecipitation experiments confirmed interaction of CLCP1 with SEMA4B, regulation of CLCP1 protein by ubiquitination and proteasome degradation enhanced in the presence of SEMA4B. These results are the first to indicate that CLCP1 plays a role in cell motility, whereas they also showed that at least one of its ligands is SEMA4B and that their interaction mediates proteasome degradation by CLCP1. Although the physiological role of the interaction between CLCP1 and SEMA4B remains to be investigated, this novel gene may become a target of therapy to inhibit metastasis of lung cancers.
Oncogene (2007) **26,** 4025–4031; doi:10.1038/sj.onc.1210183; published online 8 January 2007

Keywords: CLCP1; SEMA4B; lung cancer

Lung cancer is the leading cause of cancer-related death in developed countries. Despite a considerable body of knowledge regarding the molecular mechanisms of development and progression of lung cancer, most patients eventually die because of widespread metastases. Thus, it is considered important to identify the molecules that play crucial roles in cell motility/invasion and metastasis in order to significantly reduce mortality rates. For this purpose, we established a highly metastatic subline, LNM35, from the NCI-H460 human lung cancer cell line (Kozaki *et al.*, 2000), which showed upregulation of various proinflammatory cytokines and angiogenic chemotactic chemokines in comparison to a representative low metastatic clone of the parental line (Kozaki *et al.*, 2001). Based on this profiling analysis, we also identified and characterized a novel gene, *CLCP1* (CUB, LCCL-homology, coagulation factor V/VIII homology domains protein), also termed endothelial and smooth muscle cell-derived neuropilin-like molecule (*ESDN*)/discoidin, CUB and LCCL domain containing 2 (*DCBLD2*) (Kobuke *et al.*, 2001), that demonstrated upregulated expression in LNM35 as well as in a significant fraction of lung cancers, especially lymph node metastases (Koshikawa *et al.*, 2002). The *CLCP1* gene encodes a 775-amino-acid protein with structural similarities to neuropilins, cell surface receptors for vascular endothelial growth factor $(VEGF)_{165}$ and semaphorins (Koshikawa *et al.*, 2002), which were originally identified as neural axon repulsion signaling molecules active in axon guidance. Some class III semaphorins function as tumor suppressors, whereas one class IV member may promote tumor progression through induction of angiogenesis (Kruger *et al.*, 2005). In the present study, we explored the functions of CLCP1 in tumor progression and metastasis, and found that knock down reduces tumor cell motility. Using the phage peptide library, we also obtained evidence that at least one ligand of CLCP1, Sema domain of the human semaphorin 4B (SEMA4B), is a class IV semaphorin that may be also involved in the regulation of cell motility through its induction of CLCP1 degradation.

Observation of a high expression of *CLCP1* in lung cancer specimens prompted us to examine its functional contribution to the high metastatic properties of LNM35 cells. We generated several small interfering RNA (siRNA) constructs expressing short hairpin RNAs targeting CLCP1, and found two siRNA sites (siCLCP1–2 and siCLCP1–3) that were able to effectively knock down CLCP1 expression in 293T cells co-transfected with a CLCP1 expression vector and an

Correspondence: Dr H Osada, Division of Molecular Oncology, Aichi Cancer Center Research Institute, 1-1 Kanokoden, Chikusa-ku, Nagoya 464-8681, Japan.
E-mail: hosada@aichi-cc.jp
Received 5 June 2006; revised 30 October 2006; accepted 2 November 2006; published online 8 January 2007

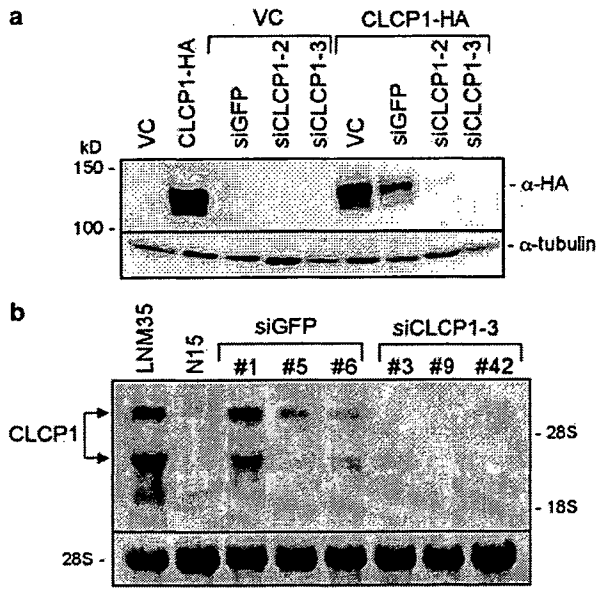

Figure 1 CLCP1 expression and establishment of LNM35-RNAi clones. (a) Immunoblotting of CLCP1-RNAi transfectants. RNAi plasmid vectors were constructed by insertion of the H1 promoter 5′ upstream of the CMV promoter driving a neomycin-resistant gene (pH1-RNA neomycin). CLCP1-RNAi sites were designed at 1196–1214 nt and 1935–1953 nt of *CLCP1* ORFs for siCLCP1–2 and siCLCP1–3, respectively. A blast homology search did not indicate any strong homology for these RNAi sites. 293T cells were transfected with each RNAi-vector along with the HA-tagged CLCP1 expression vector (Koshikawa *et al*., 2002). A control RNAi construct for the GFP gene, siGFP, was also used. Note the significant reduction of expression of CLCP1 protein observed with siCLCP1–2 and siCLCP1–3. (b) Northern blotting of stable LNM35-RNAi clones. LNM35 was transfected with siCLCP1–3 RNAi constructs and selected with neomycin (1 mg/ml) for 2 weeks. The expression of endogenous *CLCP1* transcripts was almost undetectable in the LNM35 siCLCP1–3 clones (nos. 3, 9 and 42), whereas the high level of expression of *CLCP1* was not affected in control clones that received the siGFP construct. Note the significant difference in *CLCP1* expression level between LNM35 and the parental line N15.

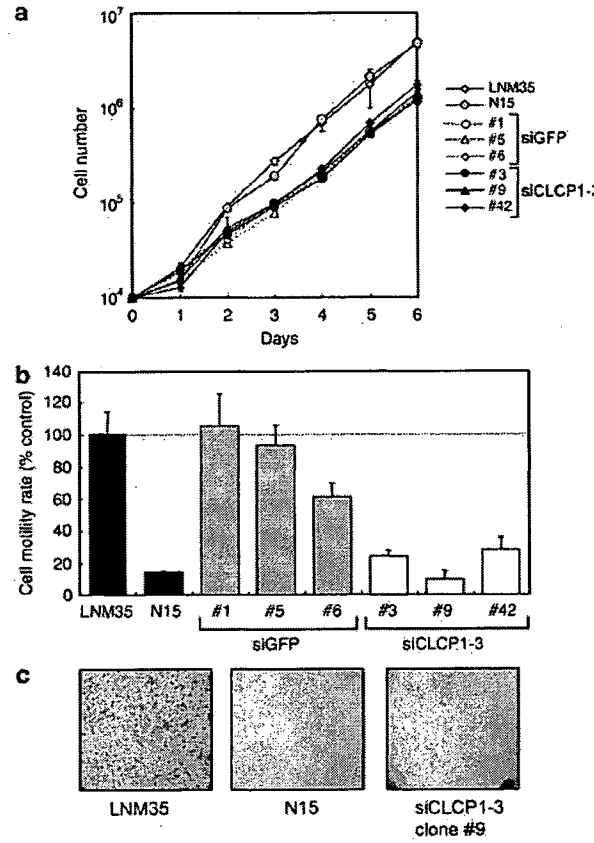

Figure 2 Cell proliferation and motility of LNM35 RNAi clones. (a) Cell proliferation assay. Stable clones were plated at 1×10^4 per dish in RPMI1640 medium with 5% fetal bovine serum and neomycin, then cell numbers were counted each day with a Z1 Coulter Counter (Beckman Coulter, Fullerton, CA, USA). The growth rates of the siCLCP1–3 clones were quite similar to those of the control siGFP clones, (b, c) *in vitro* motility assay. Motility of the RNAi clones was studied using transwell chambers, as described previously (Kozaki *et al*., 2001) and found to be significantly decreased in all three siCLCP1–3 clones (white bars), whereas the siGFP clones (hatched bars) retained their high levels of motility. (c) A number of migrated cells were observed among the LNM35 cells by Giemsa staining, whereas there were very few N15 or siCLCP1 cells (×40 magnification). The small dots represent 8 μm-sized transwell chamber pores.

siRNA vector (Figure 1a). To determine whether these findings were associated with decreased cell growth and/or motility of LNM35, we established stable LNM35 transfectant clones. Northern blotting (Figure 1b) revealed that the expression level of *CLCP1* in siCLCP1–3 clones nos. 3, 9 and 42 was significantly reduced to the level of the parental subclone of NCI-H460, N15, whereas *CLCP1* expression was not affected in control siGreen fluorescent protein (siGFP) clones (Supplementary Figure 3). Thereafter, these three siCLCP1–3 clones were employed for further biological analyses.

Cell growth rate was studied and the growth rates of the siCLCP1–3 clones were quite similar to those of siGFP clones (Figure 2a), suggesting that CLCP1 expression is not involved in the regulation of cell growth in LNM35 cells. However, motility was significantly decreased in the siCLCP1–3 clones, whereas the siGFP clones retained high motility (Figure 2b and c), implying that CLCP1 has an effect to enhance cell migration.

Concurrently with the above analyses, we searched for cell surface molecules specific to LNM35 using a phage display method in order to identify the molecular mechanisms of the high motility/invasion ability of LNM35. One of the peptides enriched with this method was SAYIPDS, whose sequence was nearly identical to that of SAYIPES within the SEMA4B gene (Figure 3a). This domain is known to be crucial for interactions with other proteins. CLCP1 has structural similarities to neuropilins, which function as cell surface receptors for semaphorins, therefore, we speculated that the selected peptide and SEMA4B might interact with CLCP1. We compared the interactions of the phage with LNM35 (high CLCP1 expression) and N15 (low CLCP1 expression). When cells were incubated with the phage displaying the

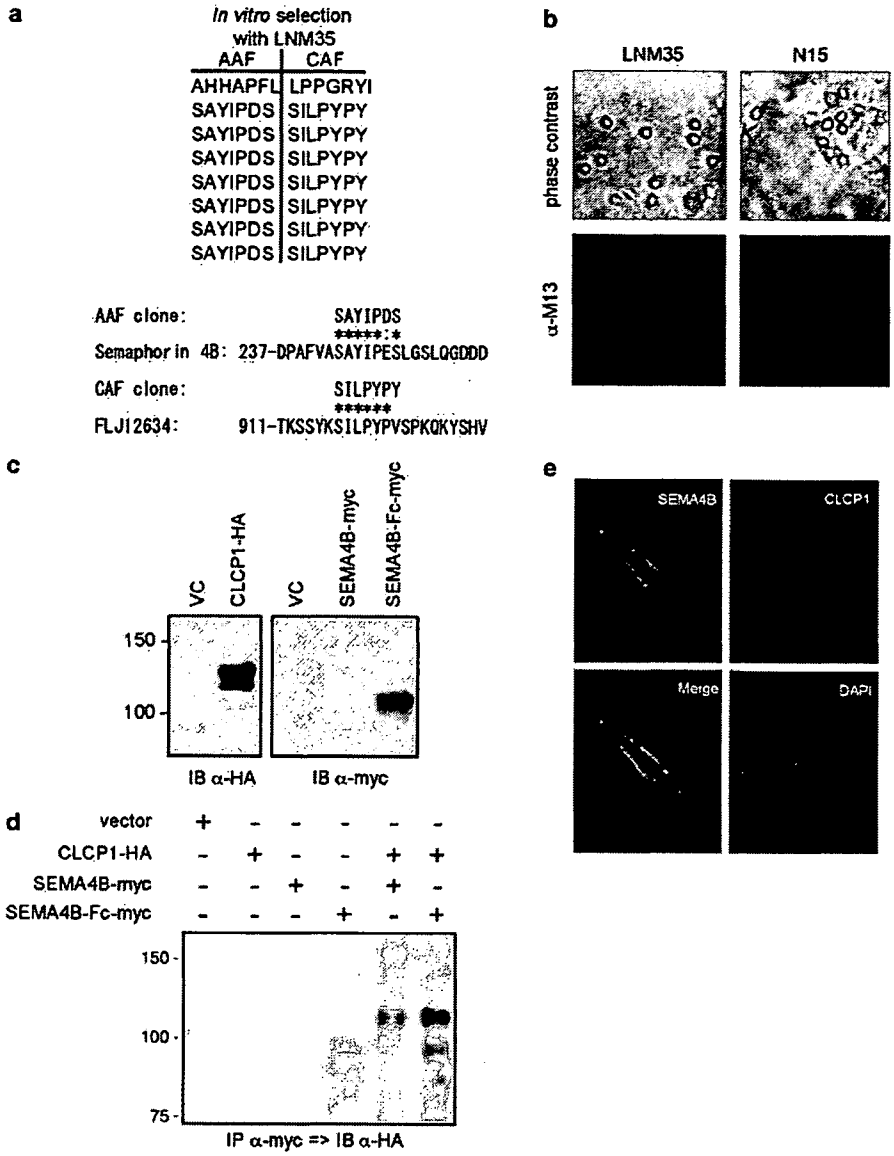

Figure 3 CLCP1 interacts with SEMA4B. (**a**) *In vitro* selection of LNM35 cells using a phage display library (PhD-7 Phage Display Peptide Library, New England Biolabs, Ipswich, MA, USA). For each selection, $1\text{–}2 \times 10^{11}$ PFU of phage particles were overlaid on LNM35 cells. After incubation and washing, attached phages were eluted with acid elution buffer (acid-associated fraction (AAF)). Tightly associated phages were also recovered after cell lysis (cell-associated fraction (CAF)). The phages were amplified following infection with bacteria and rounds of incubation-elution-amplification were repeated. Seven of the eight AAF phage clones sequenced after four rounds of selection contained the SAYIPDS peptide, which was nearly identical to the sequence SAYIPES within the SEMA4B gene. CAF phage results indicated the sequence of a hypothetical protein FLJ12634. (**b**) Immunofluorescence of phages attached to LNM35. Both LNM35 (with high CLCP1 expression) and N15 (with low CLCP1 expression) cells were incubated with phages displaying the SAYIPDS peptide. After washing and fixation, cell-attached phages were immuno-stained with the monoclonal antibody against M13 procoat protein (GE Healthcare Bio-Science, Piscataway, NJ, USA) and Alexa488-conjugated anti-mouse IgG (Invitrogen, Carlsbad, CA, USA). Note the stronger binding of the SAYIPDS phage with LNM35 as compared to that with N15. (**c**, **d**) Co-immunoprecipitation of CLCP1 with SEMA4B. The SEMA4B cDNA clone, KIAA1745, was kindly provided by Kazusa DNA Research Institute. For the SEMA4B-myc expression construct, the SEMA4B ORF was introduced into pcDNA3 (Invitrogen) together with myc-tag at its C-terminus. For the SEMA4B-Fc-myc construct, a 1720-bp *Sac*II-*Bam*HI fragment of KIAA1745 containing only the Sema domain was fused to the cDNA of the human IgG1 Fc portion in the pcDNA vector with an myc-tag at the C-terminus of the Fc portion. SEMA4B-myc or SEMA4B-Fc-myc was co-transfected with CLCP1-HA into 293T cells, and the generated proteins were immunoprecipitated with mouse monoclonal anti-myc-tag antibody 9E10. Immunoblots of these precipitates with rabbit anti-HA antibodies clearly demonstrated co-immunoprecipitation of CLCP1 with SEMA4B proteins. (**e**) Immunofluorescence of SEMA4B and CLCP1. The A549 lung cancer cell line was transfected with SEMA4B-myc and CLCP1-HA expression vectors, then stained with Alexa Fluor dye-labeled secondary antibodies (Invitrogen) after MG-132 treatment, as performed in Figure 4b and c. Observation with a confocal microscope (Olympus, Tokyo, Japan) showed both CLCP1 and SEMA4B to be mainly localized on the cell surface membrane, with colocalization clearly observed in merged images.

SAYIPDS peptide and then immuno-stained with the anti-M13 antibody against the phage particle, LNM35 staining was more intense than that of N15 (Figure 3b). Next, the indicated interaction between CLCP1 and SEMA4B was studied using an myc-tagged full-length SEMA4B construct, as well as an myc-tagged SEMA4B-Fc fusion construct consisting of the SEMA4B Sema domain and immunoglobulin (Ig)G Fc portion. After co-transfection with hemagglutinin (HA)-CLCP1 into 293T cells, anti-HA immunoblotting of anti-myc immunoprecipitates clearly demonstrated co-precipitation of CLCP1 with SEMA4B or SEMA4B-Fc (Figure 3d). Further, colocalization of CLCP1 and SEMA4B proteins on cell surface membranes was demonstrated by immunofluorescence analysis (Figure 3e).

HA-tagged CLCP1 demonstrated two sizes, 130 and 110 kDa, which were both larger than the predicted molecular mass of 80 kDa. We previously speculated that post-translational modifications such as glycosylation might account for this discrepancy (Koshikawa *et al.*, 2002), as is the case with most transmembrane proteins. To confirm this, 293T cells were transfected with HA-CLCP1 and then treated with tunicamycin, which blocks the first step in the biosynthesis of N-linked oligosaccharides. Tunicamycin treatment reduced the amounts of both the 130- and 110-kDa bands in a dose-dependent manner. Simultaneously, a novel 80-kDa band appeared (Figure 4a), indicating that CLCP1 protein is indeed post-translationally modified by glycosylation, resulting in 130- and 110-kDa-sized proteins, which might be properly processed into transmembrane proteins.

We found that the intensity of the CLCP1 protein band was significantly weaker after CLCP1-SEMA4B co-transfection as compared to with CLCP1 transfection alone (Figure 4b), and subsequently attempted to determine whether SEMA4B caused degradation of CLCP1 protein in a proteasome-dependent manner. When 293T cells were transfected with CLCP1 and/or SEMA4B, and then treated with MG-132, a specific inhibitor of proteasomes, anti-HA immunoblots indicated an increased intensity of both the 130- and 110-kDa bands in the CLCP1 transfectants (Figure 4b, lanes 3 and 4), suggesting that CLCP1 alone was originally regulated by proteasome degradation. However, CLCP1–SEMA4B and CLCP1–SEMA4B-Fc co-transfection were both associated with a significantly reduced intensity of the largest band (130 kDa) (Figure 4b, lanes 5 and 7). Similarly, MG-132 treatment enhanced the intensity of the 110-kDa band (Figure 4b, lanes 4, 6 and 8). However, the 130-kDa band was only moderately restored with CLCP1–SEMA4B co-transfection (Figure 4b, lane 6) and not recovered at all with CLCP1–SEMA4B-Fc co-transfection (Figure 4b, lane 8). In Figure 4c, the size of the co-immunoprecipitated CLCP1 isoform was compared with that of CLCP1 proteins in cell lysates derived from transfectants treated with or without MG-132 or another proteasome inhibitor, lactacystin, which was effective for a Smad4 mutant (Yanagisawa *et al.*, 2000) (Supplementary Figures 1 and 2). The main co-precipitated CLCP1 isoform appeared to be a 110-kDa isoform, even in samples treated with proteasome inhibitors. These findings suggest that the degradation of the 130-kDa band induced by SEMA4B proteins may be too severe to be inhibited by the applied concentration of MG-132. Nevertheless, even with higher concentrations of proteasome inhibitors, full restoration of the 130-kDa band was not obtained (Supplementary Figure 2), suggesting that the interactions with SEMA4B proteins, especially SEMA4B-Fc, may not only induce degradation, but also affect full glycosylation of CLCP1. We also examined the ubiquitination status of CLCP1 using P4D1 monoclonal antibodies that recognize both monoUb and polyUb (Figure 4d). Although ubiquitinated CLCP1 was readily detected in cells co-transfected with the empty vector (Figure 4d, lane 4), the ubiquitination of CLCP1 was significantly increased following co-transfection with SEMA4B (Figure 4d, lane 6). These results suggest that CLCP1–SEMA4B interactions induce significant degradation of CLCP1 proteins, especially 130-kDa fully-glycosylated CLCP1.

This present results indicated that the neuropilin-like protein CLCP1 is upregulated in highly metastatic lung cancer cells and may promote cell motility, possibly resulting in promotion of metastasis. We also found that SEMA4B is a possible ligand of CLCP1, as CLCP1–SEMA4B interaction caused CLCP1 degradation. CLCP1/ESDN was also reported to be expressed by vascular smooth muscle cells, as well as upregulated by platelet-derived growth factor-BB stimulation and vascular injury, suggesting that it modulates growth-promoting signals (Kobuke *et al.*, 2001). Class III semaphorins interact with neuropilins through binding of their Sema and CUB or FV/VIII domains, respectively. Although the interaction domains of CLCP1 and SEMA4B have yet to be determined, it is conceivable that the Sema domain of SEMA4B interacts with CUB and FV/VIII domains of CLCP1. The fact that the sequence within the Sema domain was enriched with the phage display selection in LNM35 expressing CLCP1 provides support for this speculation.

Cell migration is a multistep process that includes leading edge protrusion, focal contact formation and actomyosin-dependent cell contraction, and also involves small guanosine triphosphatase (GTPase) and integrins. Small GTPases, including Rho, Rac and Cdc42, control cell motility by regulating actin and microtubule dynamics (Friedl and Wolf, 2003). Semaphorins and neuropilins make protein complexes with plexins, which regulate the activities of small GTPases through interactions with these small GTPases and Rho-guanine nucleotide exchange factor (Kruger *et al.*, 2005). In addition, a recent report showed that Sema4D-plexin-B1 interaction downregulates R-Ras activity through the endogenous GTPase-activating protein activity of plexin-B1, resulting in inhibition of focal contact mediated by integrins (Oinuma *et al.*, 2004). Therefore, to understand the molecular mechanisms underlying the regulation of cell motility by CLCP1, it is important to clarify whether CLCP1 signaling has any effects on the activities of these small GTPases and integrins.

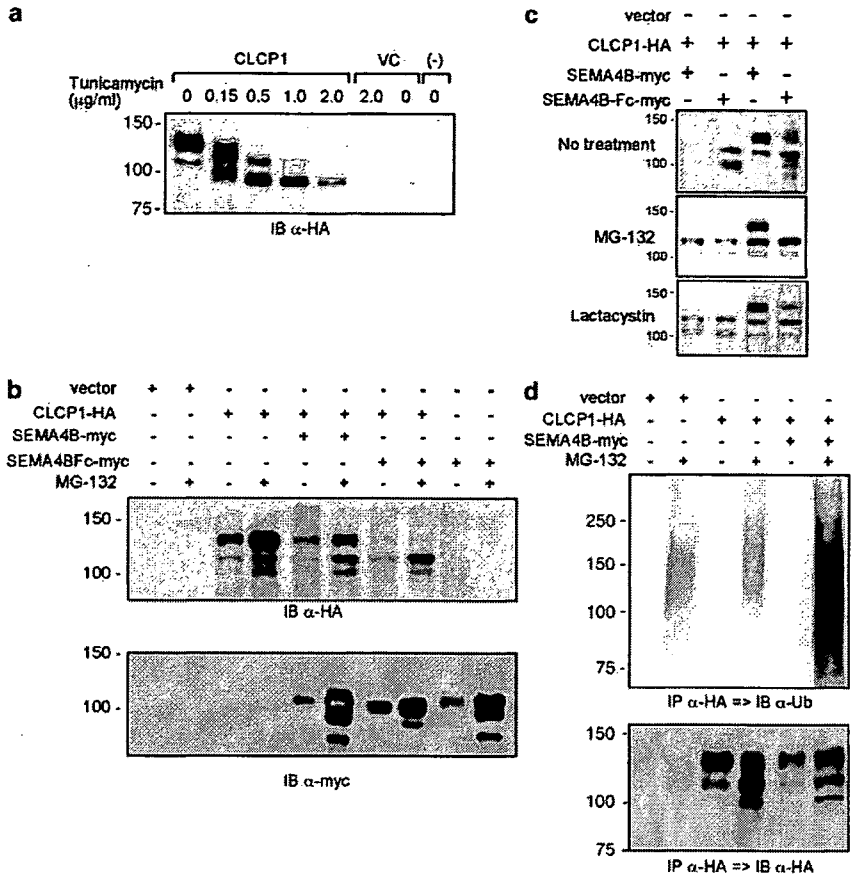

Figure 4 Post-translational modification of CLCP1 protein. (**a**) *N*-glycosylation of CLCP1. 293T cells were transfected with the CLCP1-HA vector and then treated with an *N*-linked glycosylation inhibitor, tunicamycin (Wako Pure Chemical Industries Ltd., Osaka, Japan), for 24 h at the indicated concentrations. Reductions in the amounts of both the 130- and 110-kDa bands resulted, with simultaneous appearance of a novel 90-kDa band similar to the predicted size in a dose-dependent manner. (**b**) Degradation of CLCP1 protein. 293T cells were transfected with CLCP1-HA, SEMA4B-myc and/or SEMA4B-Fc-myc, then treated with a proteasome inhibitor, MG-132 (SIGMA-ALDRICH, St Louis, MO, USA), at 10 μM for 24 h. The expression levels of CLCP1 and SEMA4B proteins were then investigated using anti-HA and anti-myc antibodies. Without MG-132 treatment, the CLCP1 protein band was significantly weaker after CLCP1/SEMA4B or CLCP1/SEMA4B-Fc co-transfection (lanes 5, 7) than with CLCP1 transfection alone (lane 3). MG-132 treatment enhanced the intensity of the CLCP1 protein band in co-transfections (lanes 6, 8) and also with CLCP1 transfection alone (lane 4). Proteasome-dependent degradations of SEMA4B proteins were also observed. (**c**) Analysis of the co-immunoprecipitated isoform of CLCP1. Immunoprecipitation and immunoblotting of CLCP1/SEMA4B and CLCP1/SEMA4B-Fc co-transfected cells were conducted, the same as in Figure 3d. Transfected cells were treated with MG-132 (10 μM) or another proteasome inhibitor, lactacystin (15 μM, Wako Pure Chemical Industries Ltd.). Immunoprecipitated proteins (lane 1, 2) were run with cell lysates before immunoprecipitation (lane 3, 4). The main immunoprecipitated CLCP1 isoform appeared to be the same 110-kDa isoform noted in (**a**). (**d**) Ubiquitination of CLCP1. As in (**b**), 293T cells were transfected and treated with MG-132. Then, CLCP1 protein was immunoprecipitated with the anti-HA antibody and analysed with the anti-ubiquitin antibody, P4D1 (Santa Cruz Biotechnology, Inc., Santa Cruz, CA, USA). Ubiquitination of CLCP1 was readily detected following transfection of CLCP1 alone (lane 4) and significantly increased by co-transfection with SEMA4B (lane 6).

In a previous study, SEMA3A inhibited the migration and spread of a breast cancer cell line, MDA-MB-231, which expresses neuropilin-1 and plexin-A1, whereas another ligand of neuropilin-1, $VEGF_{165}$, was shown to compete with SEMA3A and abrogate its inhibitory effect (Bachelder *et al.*, 2003). CLCP1 may also interact with other ligand molecules, which might regulate cell motility in competition with SEMA4B. In the present study, we also examined the involvement of cyclooxygenase 2 (COX-2) in *CLCP1* expression (Supplementary Figure 4), because a previous study showed that COX-2 was upregulated in LNM35 cells and contributed to their highly metastatic characteristics (Kozaki *et al.*, 2000). We found that nimesulide, a COX-2 inhibitor, repressed *CLCP1* mRNA levels, suggesting a functional association between COX-2 activation and *CLCP1* overexpression in LNM35 cells.

SEMA3B and *SEMA3F*, which are localized at the 3p21.3 locus, are frequently deleted in lung cancers and have been found to suppress tumor cell proliferation (Tse *et al.*, 2002; Xiang *et al.*, 2002; Castro-Rivera *et al.*, 2004). In contrast, class IV semaphorins do not show

such a tumor suppressor function, whereas Sema4D was originally reported to promote B-cell survival and T-cell activation. Another study showed that Sema4D induces angiogenesis, which was mediated by the coupling of its high-affinity receptor plexin-B1 with the Met tyrosine kinase (Conrotto *et al.*, 2005). In addition, class IV semaphorins frequently have PDZ {PSD (postsynaptic density protein) 95, DlgA (Discs large A), and ZO (zonula occludens) 1)} domain-binding motifs at their C-termini, through which they may function as receptors by mediating signal transfers through their intracellular domains. SEMA4B, 4C and 4F have been shown to interact with the PDZ domains of PSD-95 (Inagaki *et al.*, 2001; Burkhardt *et al.*, 2005), whereas SEMA4D was found to associate with CD45 protein tyrosine phosphatase (Herold *et al.*, 1996). Therefore, SEMA4B might function as a CLCP1 receptor. Sema3A–neuropilin interactions induce neuropilin-1 endocytosis, which is mediated by L1-CAM (Fournier *et al.*, 2000; Castellani *et al.*, 2004), which in turn modulates growth cone sensitivity to semaphorin repulsion signals. CLCP1 degradation after CLCP1–SEMA4B interaction may indicate an induction of CLCP1 endocytosis by SEMA4B.

In conclusion, the present results indicate that CLCP1 and its interactions with ligands including SEMA4B may become molecular targets for therapeutic inhibition of metastasis. In addition to CLCP1-siRNA, the suppression of CLCP1 functions with dominant-negative CLCP1 or negatively regulating ligands might inhibit *in vitro* motility and, consequently, *in vivo* metastasis of cancer cells. Fine mapping of the interacting regions between CLCP1 and SEMA4B may indicate concrete molecular targets. Although a full understanding of the biological roles of CLCP1 and SEMA4B remains to be achieved, further investigations of CLCP1 functions should provide novel and useful strategies to improve the clinical prognosis of lung cancer patients by facilitating the suppression of metastasis.

Acknowledgements

This work was supported in part by a Grant-in-Aid for Scientific Research on Priority Areas from the Ministry of Education, Culture, Sports, Science and Technology of Japan, a Grant-in-Aid for Scientific Research (B) and (C) from the Japan Society for the Promotion of Science, and a Grant-in-Aid for the Second Term Comprehensive Ten-Year Strategy for Cancer Control from the Ministry of Health and Welfare, Japan. We thank Kazusa DNA Research Institute for the SEMA4B cDNA clone, KIAA1745.

References

Bachelder RE, Lipscomb EA, Lin X, Wendt MA, Chadborn NH, Eickholt BJ *et al.* (2003). Competing autocrine pathways involving alternative neuropilin-1 ligands regulate chemotaxis of carcinoma cells. *Cancer Res* **63**: 5230–5233.

Burkhardt C, Muller M, Badde A, Garner CC, Gundelfinger ED, Puschel AW. (2005). Semaphorin 4B interacts with the post-synaptic density protein PSD-95/SAP90 and is recruited to synapses through a C-terminal PDZ-binding motif. *FEBS Lett* **579**: 3821–3828.

Castellani V, Falk J, Rougon G. (2004). Semaphorin3A-induced receptor endocytosis during axon guidance responses is mediated by L1 CAM. *Mol Cell Neurosci* **26**: 89–100.

Castro-Rivera E, Ran S, Thorpe P, Minna JD. (2004). Semaphorin 3B (SEMA3B) induces apoptosis in lung and breast cancer, whereas VEGF165 antagonizes this effect. *Proc Natl Acad Sci USA* **101**: 11432–11437.

Conrotto P, Valdembri D, Corso S, Serini G, Tamagnone L, Comoglio PM *et al.* (2005). Sema4D induces angiogenesis through Met recruitment by Plexin B1. *Blood* **105**: 4321–4329.

Fournier AE, Nakamura F, Kawamoto S, Goshima Y, Kalb RG, Strittmatter SM. (2000). Semaphorin3A enhances endocytosis at sites of receptor-F-actin colocalization during growth cone collapse. *J Cell Biol* **149**: 411–422.

Friedl P, Wolf K. (2003). Tumour-cell invasion and migration: diversity and escape mechanisms. *Nat Rev Cancer* **3**: 362–374.

Herold C, Elhabazi A, Bismuth G, Bensussan A, Boumsell L. (1996). CD100 is associated with CD45 at the surface of human T lymphocytes. Role in T cell homotypic adhesion. *J Immunol* **157**: 5262–5268.

Inagaki S, Ohoka Y, Sugimoto H, Fujioka S, Amazaki M, Kurinami H *et al.* (2001). Sema4c, a transmembrane semaphorin, interacts with a post-synaptic density protein, PSD-95. *J Biol Chem* **276**: 9174–9181.

Kobuke K, Furukawa Y, Sugai M, Tanigaki K, Ohashi N, Matsumori A *et al.* (2001). ESDN, a novel neuropilin-like membrane protein cloned from vascular cells with the longest secretory signal sequence among eukaryotes, is up-regulated after vascular injury. *J Biol Chem* **276**: 34105–34114.

Koshikawa K, Osada H, Kozaki K, Konishi H, Masuda A, Tatematsu Y *et al.* (2002). Significant up-regulation of a novel gene, CLCP1, in a highly metastatic lung cancer subline as well as in lung cancers *in vivo*. *Oncogene* **21**: 2822–2828.

Kozaki K, Koshikawa K, Tatematsu Y, Miyaishi O, Saito H, Hida T *et al.* (2001). Multi-faceted analyses of a highly metastatic human lung cancer cell line NCI-H460-LNM35 suggest mimicry of inflammatory cells in metastasis. *Oncogene* **20**: 4228–4234.

Kozaki K, Miyaishi O, Tsukamoto T, Tatematsu Y, Hida T, Takahashi T *et al.* (2000). Establishment and characterization of a human lung cancer cell line NCI-H460-LNM35 with consistent lymphogenous metastasis via both subcutaneous and orthotopic propagation. *Cancer Res* **60**: 2535–2540.

Kruger RP, Aurandt J, Guan KL. (2005). Semaphorins command cells to move. *Nat Rev Mol Cell Biol* **6**: 789–800.

Oinuma I, Ishikawa Y, Katoh H, Negishi M. (2004). The Semaphorin 4D receptor Plexin-B1 is a GTPase activating protein for R-Ras. *Science* **305**: 862–865.

Osada H, Tatematsu Y, Saito H, Yatabe Y, Mitsudomi T, Takahashi T. (2004). Reduced expression of class II histone deacetylase genes is associated with poor prognosis in lung cancer patients. *Int J Cancer* **112**: 26–32.